CARAVEL

Publish open access at Caravel Press

Global Decarbonisation

Journal homepage: globaldecarbonisation.com

Technical article

Performance Analysis of Indoor CO_2 Capture Methods across Operational Contexts for Building Emissions Reduction

Yongting Shen [1]* and Hongxing Yang [2]*

[1] *Renewable Energy Research Group (RERG), Department of Building Environment and Energy Engineering, The Hong Kong Polytechnic University, HKSAR, China.*

ABSTRACT

Developing low-carbon buildings with low energy consumption and healthy indoor environments is paramount for urban decarbonization, yet it remains challenging. The challenge stems from the conflicting demands on ventilation rates for maintaining low heating, ventilation, and air-conditioning (HVAC) energy demands and high indoor air quality. Indoor CO_2 capture (ICC) technologies offer a potential solution by directly capturing indoor CO_2 rather than relying on high ventilation to expel it. The effectiveness of ICC is closely related to the involved capture methods and working environment, yet an analytical model that can articulate such an interplay is lacking, hindering contextually optimal design for broad implementation. Here, we develop an analytical ICC model applicable to different capture methods and operational scenarios, enabling contextual performance analysis across varying occupancy profiles. Results show that using capture methods with higher capture rates enables ICC to achieve greater energy savings and reduced carbon emissions, although excessive capture may consume more energy than it saves. To identify feasible working conditions, we develop phase maps of ICC's CO_2 capture rates and specific energy consumption values that can achieve net energy savings and net CO_2 emission reduction. ICC is found most effective under higher HVAC load conditions, such as in cold, hot, humid, or crowded environments. In Xi'an, China, for instance, ICC achieves average energy savings of 65.6% in winter, 37.9% in summer, and 28.5% annually, with a maximum CO_2 emission reduction of 13.4 kg/day for a medium-sized office. This study provides a framework for evaluating and optimizing ICC systems, offering insights into promoting practical and wide deployment of ICCs for reducing building carbon emissions.

ARTICLE INFO

Article History:
Received: 25 September 2025
Revised: 18 January 2026
Accepted: 09 March 2026

Keywords:
Indoor carbon capture
Building energy saving
Building emissions reduction
Urban decarbonization
Indoor air quality

Article Citation:
Shen, Y., & Yang, H. (2026). Performance Analysis of Indoor CO_2 Capture Methods across Operational Contexts for Building Emissions Reduction. Global Decarbonisation, 2(1), 1–19. https://doi.org/10.65582/gd.2026.002

1. INTRODUCTION

Buildings provide essential shields for occupants from heat, cold, and precipitation, but this comes at the cost of intensive energy consumption and carbon emissions. Building operations account for approximately 30% of global final energy use and 26% of global energy-related emissions (IEA, 2025), underscoring the

* Corresponding author. Email address: yongting.shen@connect.polyu.hk (Yongting Shen); hong-xing.yang@polyu.edu.hk (Hongxing Yang)

pivotal role in decarbonizing buildings in the global pursuit of carbon neutrality (Zuo and Zhao, 2014, Wang et al., 2021). Within the building sector, heating, ventilation, and air-conditioning (HVAC) systems are responsible for about 40% of building energy worldwide, primarily due to the need to manage latent and sensible heat loads to maintain indoor thermal comfort (Department of Climate Change, Energy, the Environment and Water, 2013). The demand for HVAC energy is projected to rise further, as a result of climate change-induced extreme weather events and the increasing prevalence of HVAC installations.

Over the years, a range of strategies have been developed to reduce building energy consumption, including the integration of renewable energy sources to reduce reliance on grid electricity (Meinardi et al., 2017, Buker and Riffat, 2015, Alim et al., 2020), and the use of functionally modified building envelopes to minimize heat gain in summer or heat loss in winter (Zhai et al., 2017, Peng et al., 2021, Adhikary et al., 2021, Li et al., 2020b, Jelle, 2011). While these strategies can lower energy use, they often ignore the simultaneous control of indoor CO_2 levels, which is crucial for occupant health (Jacobson et al., 2019). Ensuring high indoor air quality (IAQ) with low CO_2 concentrations is equally important as minimizing building energy consumption. In densely occupied spaces, respiratory CO_2 can accumulate rapidly, leading to indoor CO_2 concentrations 3-7 times higher than ambient levels and posing health risks, such as headaches, vomiting, cognitive impairment, and reduced productivity (Jacobson et al., 2019, Baus and Nehr, 2022). To avoid CO_2 buildup, HVAC systems typically increase ventilation rates to introduce fresh outdoor air and expel CO_2-rich indoor air. However, this inherently raises the latent and sensible loads on HVAC systems (Steinemann et al., 2017, Shen et al., 2024, Harrouz et al., 2022b), creating a fundamental trade-off between maintaining high IAQ and low building energy consumption. Demand-controlled ventilation (DCV) partially addresses this by adjusting outdoor air intake rates based on indoor CO_2 levels, thereby reducing HVAC energy consumption and avoiding over-ventilation during low occupancy periods (Emmerich and Persily, 2001, Lu et al., 2022, Lu et al., 2011). Nevertheless, under high occupancy conditions, the trade-off between maintaining high IAQ and low building energy consumption persists.

To resolve this trade-off, a new strategy that can maintain low indoor CO_2 concentrations with minimum ventilation rates is needed, especially for high-occupancy scenarios. Recently, direct air capture (DAC) technologies have emerged, utilizing CO_2-affinity/selective materials to separate CO_2 from low concentration situations such as the ambient air (Shindell and Rogelj, 2025, Sanz-Perez et al., 2016, Chiristoph Beuttler, 2021, Fajardy et al., 2018). The potential of DAC for achieving negative emissions has been demonstrated by life-cycle assessments (LCA) of two commercial DAC plants in Hinwil and Hellisheiði, which reported carbon capture efficiencies of 85.4% and 93.1%, respectively (Deutz and Bardow, 2021). Similarly, DAC systems coupled with carbon storage have achieved negative greenhouse gas emissions when driven by low-carbon electricity, with carbon removal efficiencies ranging from 79-91% according to an LCA study (Terlouw et al., 2021). Given that indoor CO_2 concentrations are generally higher than the atmospheric level, it is technically feasible and even more energetically effective to apply DAC technologies for capturing indoor CO_2 from an LCA perspective. This realization has driven the development of indoor CO_2 capture (ICC) technologies, establishing their fundamental feasibility for emission reduction.

ICC systems capture CO_2 directly from indoor air and recirculate CO_2-lean air, thereby reducing the need for increased ventilation. This new approach offers the potential to resolve the conflict between building energy savings and IAQ (Kim et al., 2015, Shen et al., 2024, Kim et al., 2024, Harrouz et al., 2022b), while also providing additional carbon capture benefits not achievable with other advanced ventilation methods, such as demand control ventilation (Lu et al., 2011) and personalized ventilation (Melikov et al., 2002). ICC technologies were initially developed in the 1960s for crewed spacecraft and submarines, using chemical absorbents to maintain liveable environments (Isobe et al., 2016, Shen et al., 2024). However, their application in buildings did not emerge until the 2010s, with research focusing on developing various ICC methods, improving capture capacity at indoor CO_2 concentrations, and maximizing ICC's performance in saving buildings' energy. In addition to the absorption-based ICC methods, other safer methods that avoid toxic solvents, such as adsorption-based (Shen and Yang, 2023, Thakkar et al., 2016, Chu et al., 2021, Rajan et al., 2017) and membrane-based ICC methods (Yoo et al., 2023, Kim et al., 2023) have been developed. Nevertheless, these methods continue to face challenges due to their limited capture capacity at the relatively low CO_2 concentrations characteristic of indoor air, compared to those found in flue gases.

Ongoing research has enhanced ICC's CO_2 capture capacity at the material and system levels (Shen and Yang, 2022, Harrouz et al., 2022b, Kim et al., 2024). For instance, hybrid adsorbent material has been designed to enable simultaneous physisorption and chemisorption of CO_2, effectively preventing CO_2 accumulation in enclosed vehicles (Youngmin Cho, 2013). The capture capacity of Y-type zeolites has been increased to 158 mg CO_2/g adsorbent per hour through amine impregnation (Lee et al., 2013). System-level improvements, such as the use of rotating packed bed designs, have also been shown to increase the interaction between indoor CO_2 molecules and absorbents, reducing indoor CO_2 levels from 1000 ppm to 100 ppm (Cheng and Tan, 2011). Addressing the adverse effects of indoor moisture on CO_2 capture has led to the development of more innovative solutions that can enhance capture capacity, including MOF-polymer composites for stable CO_2 adsorption performance in humid conditions (Park et al., 2021), moisture-resistant liquid-like CO_2 adsorbent that is easy to regenerate (Lee et al., 2021), and the application of hydrophobic coatings (Kim et al., 2022), nano-encapsulated solvent (Kim et al., 2021), or facile spray-coated diamine-appended MOF composites that displayed stable CO_2 capture capacity from indoor air with 60% RH (Seok Chae et al., 2021).

Moving forward, recent research has increasingly focused on evaluating the impact of ICC on reducing HVAC energy consumption in buildings. Studies have demonstrated that a CO_2 adsorption-based ventilation model can save 30% in AC cooling energy during tropical summers and 60% in heating energy during Central European winters (Kim et al., 2015). Evaluations of MOF-based ICC systems under real-time ambient and indoor environments have shown energy-saving potential of 30% and 24% for a classroom and residential house, respectively. Additionally, economic analysis indicates that the payback period for ICC technology is 6 years for high-occupancy buildings and 2 years for low-occupancy buildings (Harrouz et al., 2022b). A CO_2 capture-integrated energy recovery ventilation system equipped with a carbon capture filter has also been developed, enabling continuous CO_2 removal while reducing ventilation energy loads, with reported heating and cooling load reduction of 52.6% and 27.9%, respectively (Kim et al., 2025). However, these methods still require energy input to support the carbon capture processes, limiting the overall energy-saving potential. To address this, further advancements have explored the use of solar energy to drive ICC technologies (Gu et al., 2022, Shen et al., 2024), further enhancing their sustainability. Additionally, integrating ICC with other building functions, such as ICC-driven passive cooling systems for building-integrated photovoltaics, offers synergistic benefits, enabling simultaneous indoor CO_2 capture, electricity generation during summer, and reduced heating demand in winter (Kim et al., 2024). Despite significant progress, implementing ICC into the real world remains challenging, mainly due to the diversity of working conditions and capture methods, both of which affect ICC performances characterized by energy-saving potential and net CO_2 emission reduction. Therefore, an in-depth understanding is required to guide the feasible design of ICC systems for different scenarios, which, however, is lacking as existing studies often focus on specific capture methods and limited conditions.

Here, this study develops an analytical ICC model applicable to different carbon capture methods and working scenarios to systematically assess their impacts on ICC's overall performance. This model covers a wide range of carbon capture methods by varying the CO_2 capture rate and specific energy consumption, and it addresses different working scenarios by incorporating diverse occupancy profiles. Through parameter sweeping, we compare the performances for various ICC methods under selected scenarios and provide corresponding phase maps to guide context-specific designs that can achieve both building energy savings and net CO_2 emission reduction. Our results demonstrate the model's potential to facilitate broader and more effective implementation of ICC technologies.

2. METHODOLOGY

In this section, we describe the system design and modelling approach for the proposed ICC system, with particular emphasis on evaluating its net carbon emission reduction and energy-saving performance.

2.1. SYSTEM DESIGN

Indoor CO_2 concentration exceeding 1000 ppm may pose health risks to occupants, such as headaches, nausea, reduced cognitive function, and productivity (Jacobson et al., 2019). Levels above 10,000 ppm can be dangerous and even life-threatening (Figure 1a). In the absence of adequate ventilation, indoor CO_2 concentrations can reach values 3-7 times higher than those found outdoors. To address elevated indoor CO_2, HVAC systems typically increase ventilation rates, which substantially raises energy demand - especially when outdoor temperature and humidity differ markedly from indoor comfort standards. Conversely, reducing ventilation rates lowers energy use but does not effectively remove CO_2 from the indoor environment, resulting in a trade-off between maintaining high IAQ and minimizing building energy use (Figure 1b). To overcome this trade-off, a new strategy that allows for low ventilation rates while still sustaining safe indoor CO_2 levels is needed (Figure 1b).

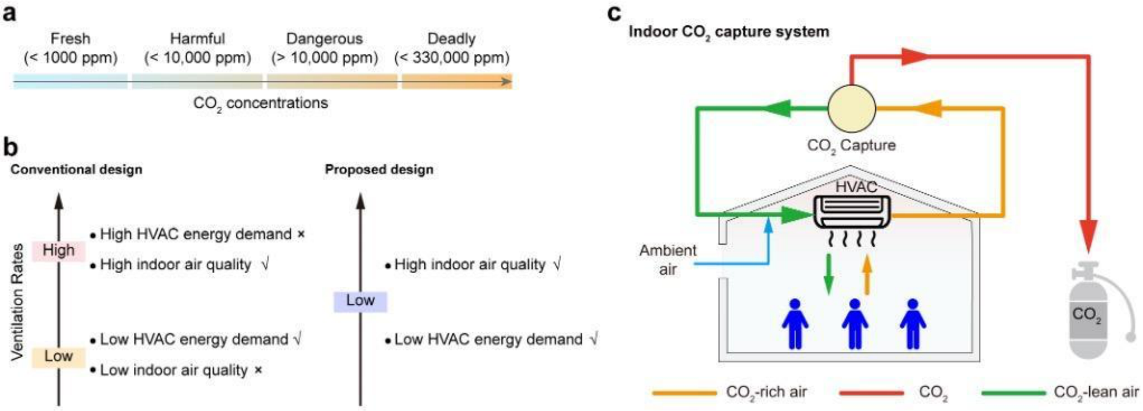

Figure 1. Conceptual design and operation of the ICC system. **(a)** Impacts of different indoor CO_2 concentration levels on human health. **(b)** The proposed ICC system addresses the trade-off in conventional HVAC design between maintaining high IAQ and minimizing building energy consumption. **(c)** Schematic illustration of the ICC system concept.

This study introduces an indoor CO_2 capture (ICC) system that uses carbon capture devices to directly remove CO_2 from stale indoor air, recirculating CO_2-depleted air to replace the intake of outdoor air. This configuration enables the ICC system to maintain high IAQ at ultra-low ventilation rates, thereby reducing building energy demand. The captured CO_2 is concentrated for subsequent storage or utilization (Figure 1c). In this work, we evaluate and compare the energy-saving potential and net CO_2 emission reduction of various ICC methods, taking into account the effects of weather conditions, CO_2 capture rates, and the specific energy consumption of carbon capture methods. The specific energy consumption refers to the energy needed to regenerate each kilogram of CO_2 and is determined by carbon capture methods and materials used. This part of the energy requirement may lead to additional CO_2 emissions, potentially offsetting the overall benefits of carbon capture (Prajapati et al., 2022, Mertens et al., 2023), requiring nuanced analysis to ensure net carbon emission reduction.

2.2. Modelling

This section describes the major modelling process for the proposed ICC system. The modelling framework is designed to quantify both energy savings and CO_2 emissions. All simulations are conducted under the condition that indoor CO_2 concentrations remain below 1000 ppm across various conditions. Notably, we assume that air filtration can be integrated into the ICC system to avoid the accumulation of potential pathogens and other air pollutants, such as volatile organic compounds. The real-time CO_2 concentration inside the room, $P_{CO_2}(t)$, is calculated as follows:

$$P_{CO_2}(t) = P_{CO_2}(t-1) + \Delta P_{CO_2}(t) \tag{1}$$

$\Delta P_{CO_2}(t)$ represents the change in indoor CO_2 concentration at each time step, which is 30 seconds in this study. This variation is calculated based on the mass conservation of CO_2 flows, while also ensuring the maintenance of indoor air pressure.

$$E_{old/new,HVAC} = E_{latent} + E_{sensible} \tag{2}$$

The total energy loads of the HVAC system E_{HVAC}, in both conventional and proposed scenarios, comprises latent and sensible components, denoted as E_{latent} and $E_{sensible}$, respectively. These heat loads are attributable to the newly introduced outdoor air and exclude potential internal heat gains from occupants or equipment, thereby isolating the energy-saving performance of ICC's reduced ventilation rates. Specifically, the latent energy load E_{latent}, can be calculated as below:

$$E_{latent} = \int_{t_{min}}^{t_{max}} \dot{m}_w \times C_w \, dt \quad (3)$$

$\dot{m}_w$ represents the amount of water added or removed by the air-conditioning (AC) system for dehumidification or humidification. It is determined by the minimum difference in water content between the newly introduced air and the standard indoor air.

$$\dot{m}_w = min\left(\left|\dot{m}_{w,amb} + \dot{m}_{w,occu} - \dot{m}_{w,standard}\right|\right) \quad (4)$$

$\dot{m}_{w,amb}$ is the water content in newly introduced ambient air, which is the sum of ventilated air, β, and infiltration air, $\dot{m}_{inf}$. $\dot{m}_{w,occu}$ is the water content generated by occupants inside (kg/s). $\dot{m}_{w,standard}$ is the water content in the standard indoor air.

$$\dot{m}_{w,amb} + \dot{m}_{w,occu} = \left[\left(\beta + \dot{m}_{inf}\right) \times \varphi_{amb}\right] / \left(1 + \varphi_{amb}\right) \quad (5)$$

φ_{amb} is the humidity ratio of ambient air, defined as the mass of water vapor per kilogram of dry air. This value is determined by the temperature and ambient pressure, as well as outdoor relative humidity (RH).

$$\dot{m}_{w,standard} = \frac{\left(\beta + \dot{m}_{inf}\right) \times \varphi_{standard}}{1 + \varphi_{amb}} \quad (6)$$

$\varphi_{standard}$ is the humidity ratio of the indoor air, which is determined by Eq.(7).

$$\varphi_{standard} = f\left(T_{standard}, P_{room}, RH_{standard}\right) \quad (7)$$

Once the minimum value of $\dot{m}_w$ is identified by the modelling, the corresponding value of $RH_{standard}$ that yields this minimum is determined. The $RH_{standard}$ value, varying between 40% to 60% for thermal comfort and minimum latent loads, can then be used to calculate $\dot{m}_{w,standard}$.

$$E_{sensible} = \int_{t_{min}}^{t_{max}} \left(\beta + \dot{m}_{inf}\right) \times C_{air} \times \Delta T \, dt \quad (8)$$

C_{air} denotes the specific heat capacity of air, and ΔT represents the temperature difference between the outdoor and indoor environments.

$$\xi = \frac{E_{old,HVAC} - E_{new,total}}{E_{old,HVAC}} \quad (9)$$

ξ represents the percentage of the energy savings achieved by the new system compared to the conventional design.

$$E_{new,total} = E_{new,HVAC} + E_{ICC} \quad (10)$$

$E_{new,total}$ denotes the total energy consumption of the proposed design, which includes both the HVAC energy consumption and the energy consumption of the ICC system.

$$m_{net,CO_2} = e_{HVAC} + e_{ICC} - m_{CO_2} \tag{11}$$

e_{HVAC} represents the CO_2 emissions associated with the energy consumed by the HVAC system (kg); while e_{ICC} denotes the penal carbon emissions from ICC operation (kg). In the conventional case, both e_{ICC} and m_{CO_2} are zero. Notably, the exhaled CO_2, which constitutes a non-trivial yet often overlooked emission sector, is captured by ICC rather than being expelled into the atmosphere by conventional methods. However, not all of the respiratory CO_2 can be captured, and the actual amount of captured CO_2, m_{CO_2}(kg), can be calculated as below:

$$m_{CO_2} = \int_{t_{min}}^{t_{max}} \dot{m}_{CO_2}\, dt \tag{12}$$

$\dot{m}_{CO_2}$ is the CO_2 capture rate (kg/s). The CO_2 emission factor used in this study, based on heat generation from natural gas and oil combustion, is 0.25 kg/kWh (Our World in Data, 2023). We also conduct parameter analysis to investigate the impacts of CO_2 emission factor on the overall ICC performance.

2.3. *Evaluation Process*

The evaluation process starts with the input of weather conditions, occupancy profiles, and performance parameters of the ICC system. In the process flow diagram (see Figure 2), the conventional scenario is represented by grey lines, while the proposed ICC scenario is indicated by blue lines. The ventilation profile is determined based on occupancy and the satisfaction of IAQ requirements, that is, the indoor CO_2 concentration should be below 1000 ppm (Wang et al., 2018, ASHRAE 62.1, 2010). This design follows the dynamic regulation of demand control ventilation (Lu et al., 2011). For the ICC case, the new ventilation profile and the amount of captured CO_2 are established according to ICC performance and occupancy profile. Using the weather conditions and ventilation profile, the sensible and latent loads for both cases are calculated to maintain thermal comfort within the indoor environment. The standard indoor temperature for summer is 25°C, and 10 ~ 20°C for winter, while the indoor RH is always maintained between 40% and 60% (Harrouz et al., 2022a), with the specific value determined by the real-time water vapor content of the outdoor air.

By comparing the HVAC loads of both scenarios, the energy savings of the HVAC system can be quantified. However, in the ICC case, there is an additional energy consumption sector associated with carbon capture, which is determined by the amount of captured CO_2 and the specific energy consumption required for the capture process.

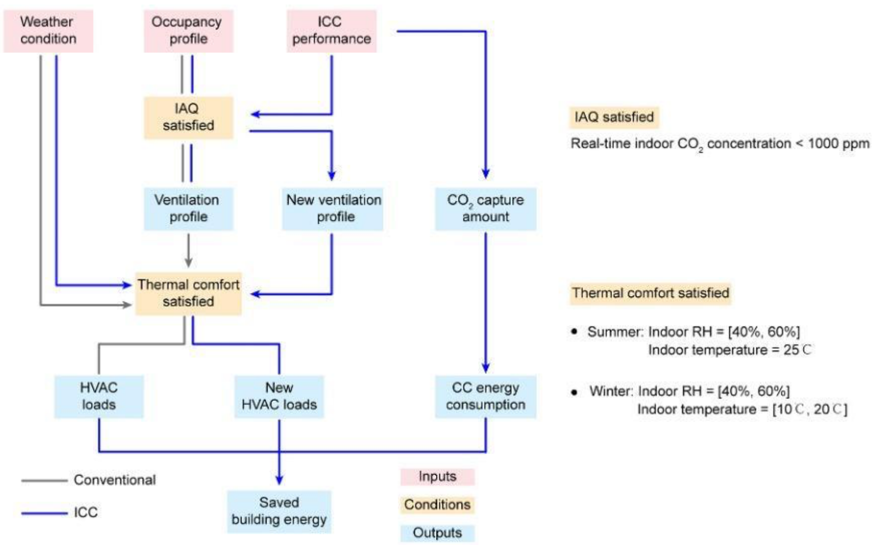

Figure 2. Logic chart of this study. All results are based on the satisfaction of both IAQ and thermal comfort requirements.

3. Working conditions

In this section, we present the working conditions of the ICC system, including indoor conditions and outdoor weather conditions. The indoor conditions typically include the occupancy profile, room sizes, and ventilation rates. For the outdoor conditions, climatic factors such as temperature and relative humidity are taken into account. In this study, the city of Xi'an, China, was selected as the case study location due to its distinct four-season climate. Specifically, Xi'an experiences hot/humid summers and cold/dry winters, representing two distinct weather conditions with high sensible and latent loads.

3.1. Indoor conditions

Occupancy patterns have a direct impact on indoor CO_2 concentration and ventilation requirements. In this study, we selected the occupancy profile of a medium office setting, which is characterized by a typical pattern of clocking in and out (Figure 3a). Notably, in this study, we assume that the office room is a well-mixed room, in which the CO_2 and other air components are uniformly distributed throughout the space within each time step. The indoor CO_2 concentration fluctuates as a result of CO_2 generation (occupant exhalation, infiltration, ventilation) and removal (ventilation, carbon capture, exfiltration). In both the conventional (no capture) and ICC cases, the indoor CO_2 concentrations are maintained below 1000 ppm to comply with IAQ standards (Figure 3b). Figure 3c presents four operational cases comparing the dynamic curves of indoor CO_2 concentration, all of which exhibit exponential build-up and decay similar to findings from other studies (Lu et al., 2011, Youngmin Cho, 2013, Lee et al., 2013, Sinha et al., 2022, Grande, 2022, Tian et al., 2023, Harrouz et al., 2023). To prevent excessive CO_2 removal, an additional constraint was imposed: ICC operation is suspended if indoor CO_2 concentration falls below 350 ppm, the lower bound of the atmospheric CO_2 level (350~450 ppm) (Kim et al., 2015, Lee et al., 2013) (Figure 3b). This measure avoids unnecessary over-capture and balances the advantages of lower CO_2 levels against the increased energy consumption associated with capturing CO_2 at concentrations already satisfying healthy IAQ. With these constraints applied, the ventilation rates for each case were calculated, as shown in Figure 3c. While ventilation rates in both cases generally follow the occupancy profile shown in Figure 3a, a marked reduction in ventilation rates is observed in the ICC case, highlighting the system's potential to significantly lower HVAC energy demand (Figure 3d).

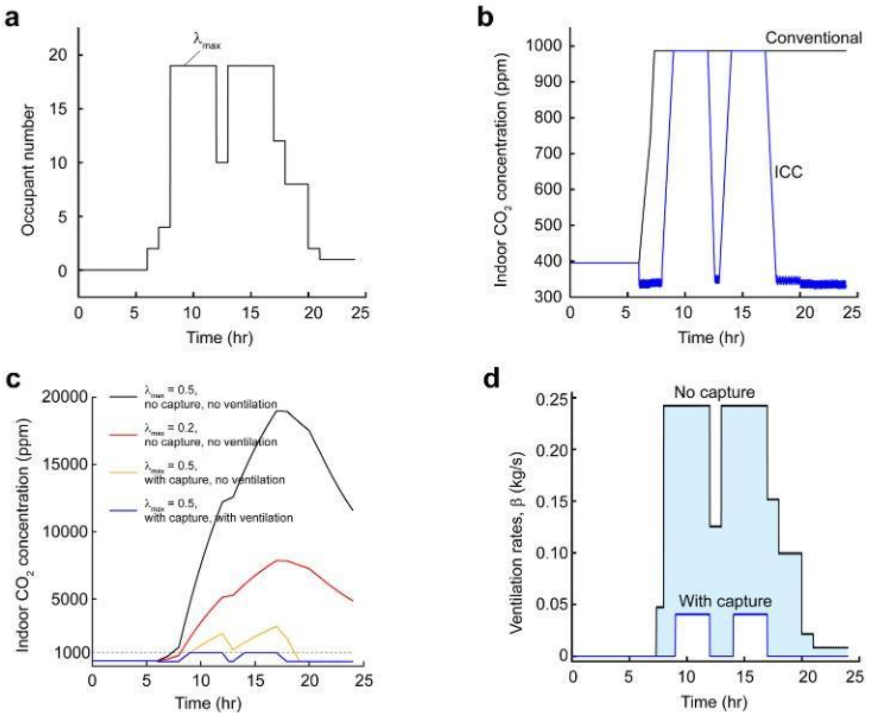

Figure 3. Working conditions of the indoor environment. **(a)** Occupancy profile over 24 hours. **(b)** Dynamic indoor CO_2 concentration, comparing the conventional and ICC case. **(c)** Comparison of indoor CO_2 concentration variation curves of four cases. **(d)** Corresponding air ventilation rates for both cases, determined by ensuring the indoor CO_2 concentration is below 1000 ppm.

3.2. Weather Conditions

In this section, we present the weather conditions in Xi'an during the hottest and coldest months, July and January, respectively, as well as their implications for building energy loads. Xi'an experiences hot and humid summers (Figure 4a), while in January, temperatures frequently and largely drop below 10°C (Figure 4b), and the relative humidity (RH) is significantly lower compared to July. Consequently, the latent load is more prominent in July due to higher humidity, whereas in January, the sensible load – primarily for heating the space - is more prominent than that in July. To maintain indoor comfort, RH is kept between 40 and 60%. Seasonal indoor temperature settings are applied: heating is provided in winter when outdoor temperatures fall below 10°C, with an indoor setpoint of 20°C, and cooling is applied in summer when outdoor temperature exceeds 25°C. Regardless of the season, humidification and dehumidification are applied when outdoor RH is below 40% and above 60%, respectively. The indoor RH setpoint is selected between 40% ~ 60% and is determined by the minimum difference in water vapor content between indoor and outdoor air.

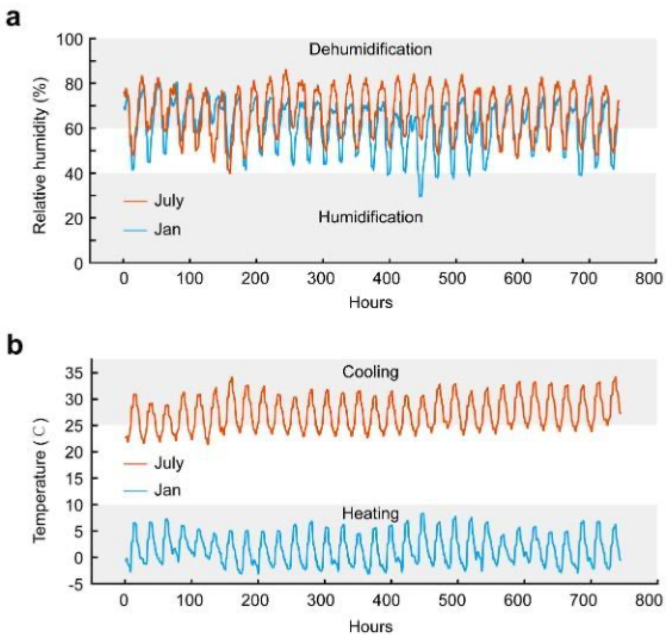

Figure 4. Weather conditions in Xi'an. **(a)** RH in Xi'an during July and January (31 days each). **(b)** Dry bulb temperature in Xi'an during July and January (31 days each).

4. Results

This study focuses on the comparative analysis of energy-saving performance and CO_2 emission reduction between the conventional HVAC case and the ICC case, as well as among different capture methods distinguished by their specific energy consumption and capture rates. By systematically evaluating these factors, the study aims to identify effective ICC system designs for reducing building energy demand and net CO_2 emissions.

4.1. Energy Saving Performance

This section investigates the net energy-saving performance of the ICC system, which is defined as the difference between the reduction in building HVAC energy consumption and the energy consumed to operate the ICC device. Energy loads are evaluated on hourly, daily, and monthly timescales to capture dynamic variations. As illustrated in Figure 5, the sensible and latent loads for July – calculated based on the medium office occupancy profile and the satisfaction of indoor CO_2 concentrations below 1000 ppm, demonstrate a clear reduction in the ICC case compared to the conventional scenario.

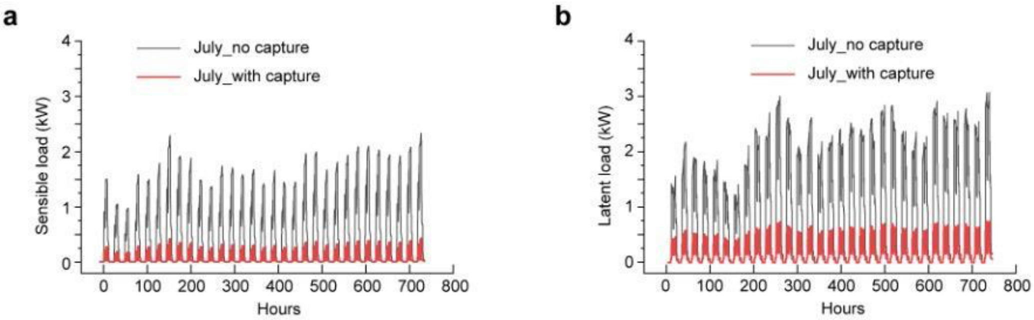

Figure 5. Dynamic HVAC energy loads in July. **(a)** Sensible loads, comparing between the conventional case (no capture) and the ICC case. **(b)** Latent loads in July.

Figure 6 evaluates the impact of ICC implementation on mean hourly sensible and latent energy loads during the peak summer and winter months. The analysis compares scenarios with and without ICC for both July and January, revealing that the ICC case consistently achieves lower energy loads across both periods. The shaded areas in the subfigures highlight the magnitude of energy savings achieved by ICC. For instance, in Figure 6a, the daily total sensible load in July is 12.7 kWh for the conventional case and 1.6 kWh for the ICC case. In Figure 6b, the daily total latent load in July is 22.9 kWh for the conventional case, and 4.9 kWh for the ICC case. In January, the daily total of sensible load is 41.4 kWh for the conventional case, and 5.3 kWh for the ICC case (Figure 6c), while the daily total latent load is 17.3 kWh for the conventional case and 1.3 kWh for the ICC case (Figure 6d). These comparative results underscore the substantial energy-saving potential of ICC in months with high HVAC loads.

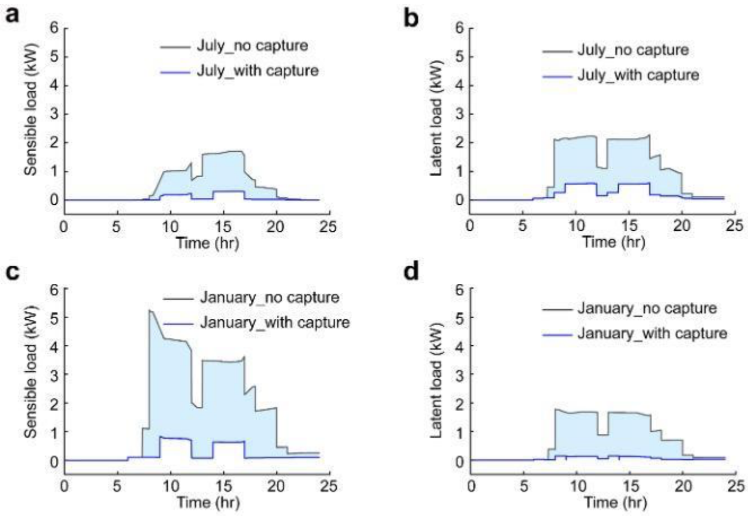

Figure 6. The 24-hr curve of sensible and latent heat loads of mean July and January. **(a)** Sensible loads in July. **(b)** latent loads in July. **(c)** Sensible loads in January. **(d)** Latent loads in January.

Figure 7 presents the monthly variation in daily total energy loads under ICC operation, using a CO_2 capture rate of 0.18 g/s. The specific energy consumption for this section of the case study is assumed to be 6 MJ/kg, which is consistent with values reported in DAC studies that typically range from 5.25 to 6.7 MJ/kg for atmospheric CO_2 capture (Zhu et al., 2021, Deutz and Bardow, 2021, Baciocchi et al., 2006, Keith et al., 2018, Sabatino et al., 2020). Notably, the minimum separation work of direct air capture methods is 19~21 kJ/mol (0.43~0.45 MJ/kg) (Siegelman et al., 2021). To facilitate comparison between different capture methods, we assume that the CO_2 capture rates are constants for the same occupancy profiles, without periodic fluctuations from capture-release cycles, such as those seen in membrane-based capture methods. For capture methods involving capture-release cycles, stable capture rates can be achieved through capture device designs, such as multi-chamber configurations and active capture control. Figure 7a presents the daily totals for each of the 31 days in July and January. The results indicate that, in July, more than half of the HVAC energy consumption is attributed to overcoming the latent load due to the high ambient RH in July in Xi'an. In contrast, in January, the dry conditions mean that latent energy is primarily used for humidification, while a greater portion of HVAC energy is consumed to overcome the sensible heat loads of the ambient air. Overall, the ICC system achieves substantial energy savings, reducing total energy consumption by 67.5% in July and 46.5% in January, after accounting for the energy required to operate the ICC device, as shown in Figure 7b. These findings highlight the significant seasonal variability in the energy-saving potential of ICC, with benefits more pronounced in periods when outdoor RH and temperature deviate substantially from indoor comfort standards.

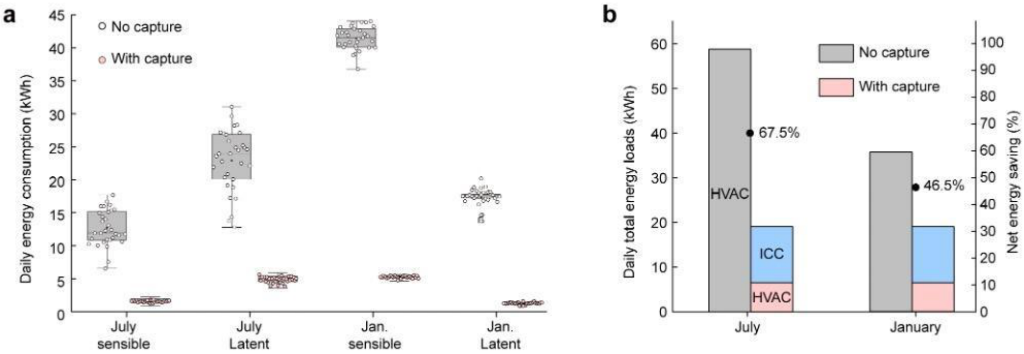

***Figure 7*. (a)** Box plot of daily total energy loads for July and January. The box represents the 25th-75th percentiles, the centre line denotes the median, and the square point denotes the mean value. Whiskers denote the full data range with the interquartile range, while the circles represent individual measurements (n = 31). **(b)** Total energy loads and energy saving potential of ICC systems compared to conventional cases.

As shown in Figure 8a-b, the energy-saving potential of ICC is higher during periods of high original energy demand. For instance, the average energy-saving potential from December to February reaches 65.6%, while in July and August, it is 37.9%. Conversely, in months with low HVAC energy demands, the energy-saving potential of ICC diminishes or becomes negative due to the additional energy consumed for CO_2 capture. For example, in April, the conventional case consumes 7.5 kWh daily, whereas the ICC case requires 13.25 kWh/day (0.72 kWh for HVAC and 12.53 kWh for CO_2 capture). In contrast, January exhibits the highest energy savings, with the conventional case consuming 59.6 kWh/day, and the ICC case consuming 19.2 kWh/day in total, resulting in a reduction of 67.8%. Despite negative savings in certain months, the annual average energy-saving potential remains substantial at 28.5%, further complemented by the carbon capture benefits provided by ICC.

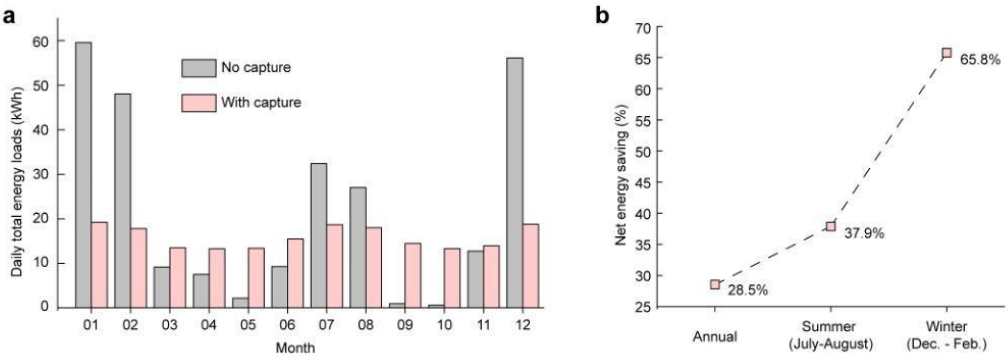

***Figure 8*. (a)** Daily total energy loads for each month, comparing the conventional case and the proposed ICC case. **(b)** Net energy saving for summer, winter, and the annual average.

4.2. Net CO_2 emission reduction

To further investigate the impacts of different CO_2 capture methods on net CO_2 emission reductions, we evaluate and compare the corresponding CO_2 emissions based on the energy loads and the CO_2 emission factor. For the conventional case, CO_2 emissions are solely attributed to HVAC operation, calculated as $e_{old,HVAC}$. With a CO_2 emission factor, δ, of 0.25 kg/kWh, a peak emission of 14.9 kg/day is reached in January, while the lowest emission is 0.15 kg/day in October. Notably, in May, September, and October, the daily CO_2 emissions for the conventional case fall below 1 kg/day due to low HVAC energy demands. In the ICC case, total CO_2 emission from both HVAC and ICC operation averaged around 4 kg/day across months. Although this value exceeds that of the conventional case in certain months, it is offset by the amount of CO_2 captured

m_{CO_2}, which is approximately 7.52 kg/day. As a result, the net CO_2 emission for the ICC case, m_{net,CO_2}, is negative (as shown in Figure 9), demonstrating the strong decarbonization potential of the ICC system.

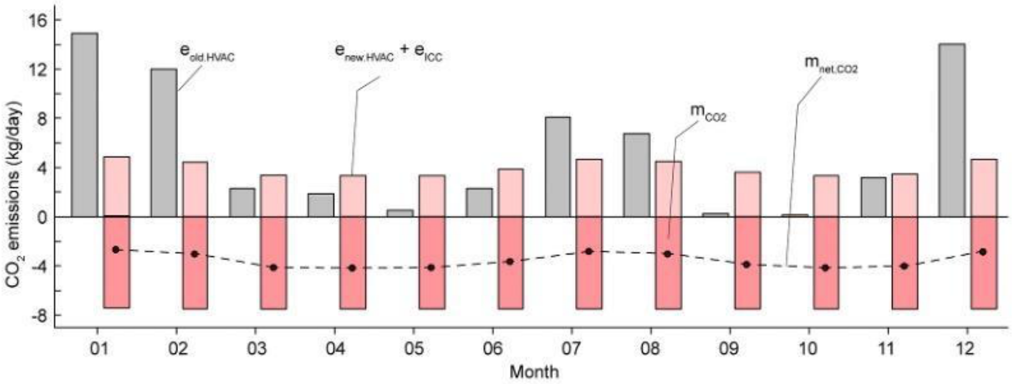

Figure 9. The CO_2 emission sectors of each month. Negative values represent CO_2 emission reduction.

Here, we examine the combined impacts of climate conditions and CO_2 capture speed, $\dot{m}_{CO_2}$, on buildings' net energy savings and CO_2 emissions reduction. A capture rate of 0 ($\dot{m}_{CO_2}$ = 0) represents the conventional case without CO_2 capture. During months with high HVAC energy consumption - such as January, February, July, August, and December – all non-zero $\dot{m}_{CO_2}$ cases exhibit lower daily total energy loads compared to the conventional case. During these periods, increasing the CO_2 capture rates leads to greater energy savings, primarily due to reduced ventilation requirements; however, the incremental benefits gradually level off as $\dot{m}_{CO_2}$ continue to increase. This occurs because increasing $\dot{m}_{CO_2}$ further reduces the HVAC subsystem's ventilation demand and associated energy use, but also raises the ICC's own energy consumption. When $\dot{m}_{CO_2}$ becomes excessive, the additional energy consumed by the ICC may outweigh the energy savings in the HVAC subsystem, thereby diminishing or even negating the overall energy-saving benefit. For instance, the annual average daily energy consumption decreases from 22.11 to 17.03 kWh/day, and 15.81 when $\dot{m}_{CO_2}$ increases from 0 to 0.12 and 0.18 g/s, respectively. However, further increasing $\dot{m}_{CO_2}$ to a larger value, i.e., 0.24 g/s, the daily energy demand rises again to 16.39 kWh/day (see Table 1). This rebound occurs because, while a higher $\dot{m}_{CO_2}$ reduces HVAC loads, they also increase the energy consumption of the ICC system, partially offsetting the overall energy savings (Figure 10a).

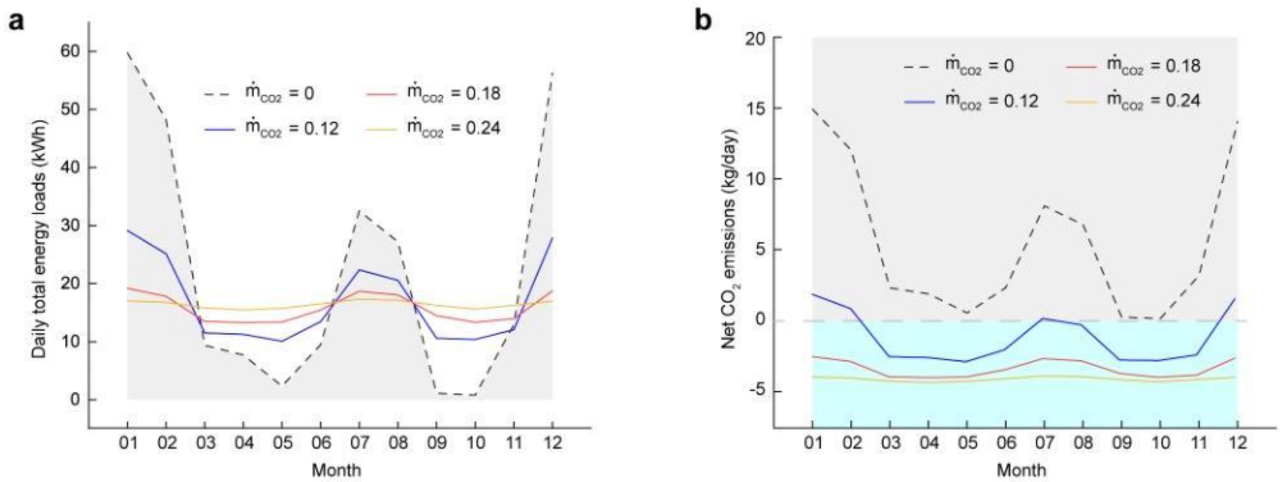

Figure 10. **(a)** Daily total energy loads. **(b)** Net CO_2 emissions of each month, under varying CO_2 capture rates.

Table 1. The annual average daily total energy loads and net CO_2 emissions for different $\dot{m}_{CO_2}$ cases. $\dot{m}_{CO_2} = 0$ means the conventional case.

Values	**Daily total energy loads (kWh/day)**				**Net CO_2 emissions (kg/day)**			
$\dot{m}_{CO_2}$ (g/s)	0	0.12	0.18	0.24	0	0.12	0.18	0.24
Average	22.11	17.03	15.81	16.39	5.52	-1.34	-3.57	-4.32

In months with low HVAC energy demand, such as April, May, and October, the daily energy consumption of the conventional case, $E_{old,HVAC}$, is actually lower than that of the ICC case, $E_{new,total}$. This is because the ICC system continues to consume energy for capturing indoor CO_2, even when HVAC loads are minimal (see Figure 10a). Despite the higher energy use in these months, the net CO_2 emission of the ICC, m_{net,CO_2}, remain significantly lower - or even negative - compared to the conventional case (Figure 10b). For instance, for the case $\dot{m}_{CO_2}$= 0.12 g/s, the net CO_2 emission in January is 1.7 kg/day for the ICC case, compared to 14.9 kg/day for the conventional case. When $\dot{m}_{CO_2}$ increases to 0.18 g/s, the net CO_2 mission drops further to -2.7 kg/day. This demonstrate that, even in months where energy savings are limited or negative, the ICC system still offers substantial benefits in terms of CO_2 emission reduction.

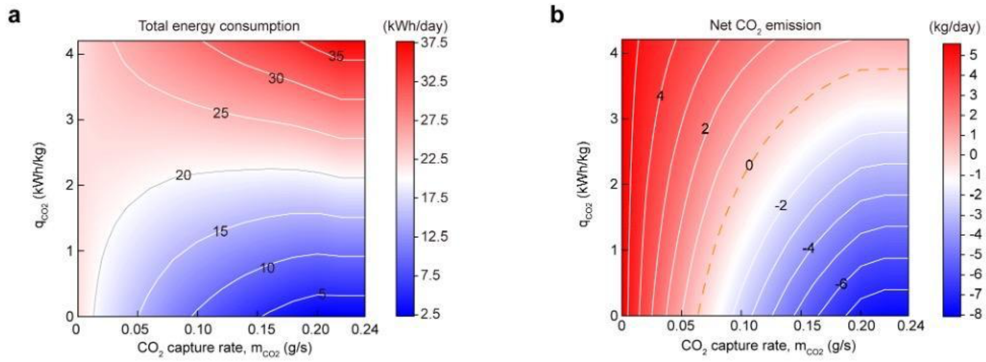

Figure 11. **(a)** Heat maps of total energy consumption. **(b)** Net CO_2 emissions under the influence of CO_2 capture rates and the specific energy consumption of CO_2 capture method, with $\lambda_{max} = 0.5$. $\dot{m}_{CO_2} = 0$ means the conventional no capture case.

To investigate the impacts of different CO_2 capture methods on energy-saving performance, we identify a specific CO_2 capture method using two key indexes: specific energy consumption and CO_2 capture rate. In Figure 11, we examine the combined impacts of the specific energy consumption of CO_2 capture (q_{CO_2}) and $\dot{m}_{CO_2}$ on yearly total energy consumption ($E_{new,total}$) and net CO_2 emissions (m_{net,CO_2}). In this study, we design q_{CO_2} to span from 0 to 4.17 kWh/kg based on literature-reported results (Goeppert et al., 2012, Zhu et al., 2021, Keith et al., 2018, Li et al., 2020a, Gu et al., 2022, Deutz and Bardow, 2021, Baciocchi et al., 2006, Sabatino et al., 2020) to cover as many capture methods and materials as possible. For the conventional case, the average daily total energy consumption is 22.11 kWh/day, with a corresponding net CO_2 emission of 5.5 kg/day. For the ICC system, $E_{new,total}$ generally increases as q_{CO_2} increases, but decreases as $\dot{m}_{CO_2}$ rises. Notably, for high q_{CO_2} cases, such as those higher than 2.5 kWh/kg, $E_{new,total}$ actually increases with higher $\dot{m}_{CO_2}$ (Figure 11a). For example, when q_{CO_2} is 1.1 kWh/kg, $E_{new,total}$ decreases from 20.3 to 11.6 kWh per day as $\dot{m}_{CO_2}$ increases from 0.02 g/s to 0.2 kg/s. In contrast, when q_{CO_2} = 3.34 kWh/kg, $E_{new,total}$ increases from 22.5 to 24.2 kWh/day over the same range of $\dot{m}_{CO_2}$ This trend occurs because, at low q_{CO_2} increasing $\dot{m}_{CO_2}$ leads to significant reduction in HVAC ventilation rates, resulting in substantial energy savings and a decrease in $E_{new,total}$. However, when the ICC method relies on processes with high specific energy consumption, the energy required for ICC outweighs the savings from reduced HVAC loads, causing $E_{new,total}$ to rise. Thus, the effectiveness of ICC in reducing $E_{new,total}$ depends critically on the specific energy consumption of the chosen CO_2 capture method.

In Figure 11b, we discuss the relationships between net CO_2 emissions, $\dot{m}_{CO_2}$ and q_{CO_2}. m_{net,CO_2} demonstrates a negative correlation with $\dot{m}_{CO_2}$ and a positive correlation with q_{CO_2}. For instance, at q_{CO_2} = 1.67 kWh/kg, net CO_2 emissions decrease from 4.0 to -4.1 kg/day as $\dot{m}_{CO_2}$ increases from 0.02 to 0.2 g/s. Conversely, for $\dot{m}_{CO_2}$= 0.10 g/s, m_{net,CO_2} increases from -2.15 to 2.6 kg per day when q_{CO_2} rises from 0.28 to 4.17 kWh/kg. In Figure 11b, the "m_{net,CO_2} = 0" line marks the threshold for negative carbon emissions; regions below this line represent net carbon removal. However, the decarbonization benefit plateaus as $\dot{m}_{CO_2}$ increases, evidenced by the gradually flattening curves in Figure 11b. This trend mirrors the pattern observed in Figure 11a, and results from the interplay between reduced HVAC energy demand and increased ICC energy consumption. Therefore, it is crucial to identify the optimal $\dot{m}_{CO_2}$ that maximizes both energy savings and carbon emission reductions, balancing the benefits of reduced ventilation loads against the energy requirements of the ICC process.

Table 2. Minimum and maximum values of the total energy loads and net CO_2 emissions for different λ_{max} case.

Values	**Daily total energy loads (kWh/day)**			**Net CO_2 emissions (kg/day)**		
λ_{max}	0.2	0.5	0.8	0.2	0.5	0.8
Conventional	8.6	22.1	35.6	2.2	5.5	8.9
Min. of ICC	1.1	2.3	8.5	-3.1	-7.8	-8.3
Max. of ICC	15.3	37.5	52.3	1.5	4.8	8.1

The impacts of the maximum occupancy levels, λ_{max} on ICC's energy savings and emission reduction are also investigated. When a lower λ_{max} is applied, $E_{new,total}$ for both the conventional and ICC cases, are reduced. For instance, the minimum and maximum $E_{new,total}$ for λ_{max} = 0.2 is 1.1 and 15.3 kWh/day, while for λ_{max} = 0.8, these values increase to 8.5 and 52.3 kWh/day. Regarding net CO_2 emission, increasing λ_{max} results in a wider range of net CO_2 emission values, depending on the operating conditions of $\dot{m}_{CO_2}$ and q_{CO_2} Despite these variations, the ICC system consistently achieves greater energy savings and lower CO_2 emissions compared to the conventional case across all λ_{max} scenarios (as shown in Table 2). Specifically, compared to the conventional case, the maximum CO_2 emission reduction amount for λ_{max} = 0.2 is 5.3 kg/day, increasing to 13.3 kg/day for λ_{max} = 0.5 and reaching 17.2 kg/day for λ_{max} = 0.8.

In Figure 12, we analyse the impact of regional CO_2 emission factors φ on the net CO_2 emission performance of the ICC system. φ represents the amount of CO_2 emitted per unit of electricity generated by a power grid, reflecting both the carbon intensity and the energy mix of the electricity supply. For instance, power grids with a high penetration of renewable energy, such as those in Sichuan, Yunnan, and Qinghai in China, can have φ as low as 0.1~0.16 kg/kWh (Ministry of Ecology and Environment of the People's Republic of China 2024). In contrast, coal-dominated power grids exhibit φ values as high as around 0.73 kg/kWh, such as those in Hebei Province, China. Net CO_2 emissions of the entire system increases with higher φ across all months, due to the greater carbon intensity of the energy consumed by both the HVAC subsystem and ICC operation. For instance, in January, net CO_2 emissions rise from -5.6 kg/day to 11.7 kg/day as φ increases from 0.1 kg/kWh to 1.0 kg/kWh. On an annual basis, net CO_2 emissions increase from -6 kg/day to 8.3 kg/day.

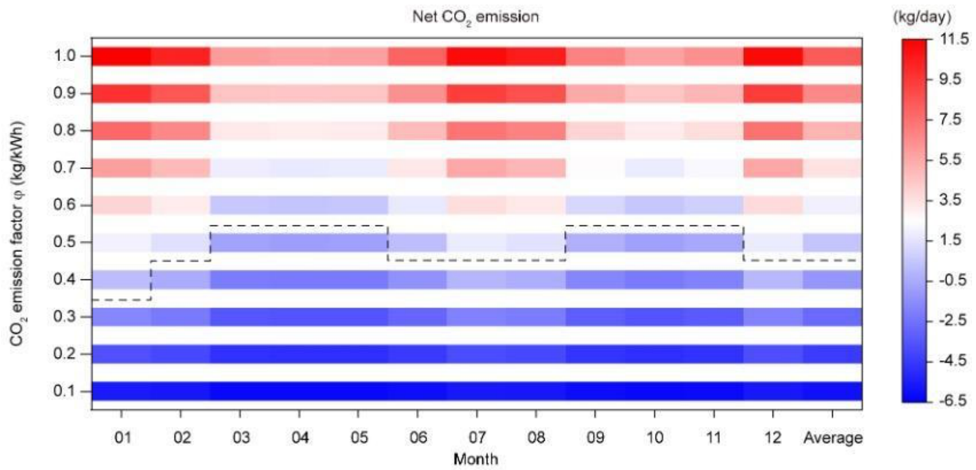

Figure 12. Net CO_2 emissions of the ICC system in different months subject to various CO_2 emission factors. The dashed black line indicates net CO_2 emission = 0.

4.3. PHASE MAP

To identify feasible operating conditions for the ICC system, we applied two criteria for the selection of $\dot{m}_{CO_2}$ and q_{CO_2}: 1) the total energy consumption of the new system ($E_{new,total}$) being lower than the HVAC energy consumption of the conventional system ($E_{old,HVAC}$), and 2) net CO_2 emission, m_{net,CO_2}, being less than 0. Figure 13 presents phase maps illustrating the combinations of q_{CO_2} and $\dot{m}_{CO_2}$ that satisfy these two criteria under different occupancy profiles and CO_2 emissions factors. In these maps, the region where $E_{new,total} < E_{old,total}$ is shaded red, while the region where $m_{net,CO_2} < 0$ is shaded blue. The overlap of these regions indicates the feasible operating domain for the ICC system, providing valuable design guidance. The phase maps are investigated for three different crowdedness scenarios, represented by varying maximum occupancy during the day: λ_{max}= 0.2 (less crowded), λ_{max} = 0.5 (crowded) and λ_{max} = 0.8 (extremely crowded). For the objective of achieving $E_{new,total} < E_{old,total}$, the feasible range of q_{CO_2} for the case φ = 0.25 kg/kWh is similar across all three λ_{max} cases, with values below 2.78 kWh/kg. This is the critical threshold for the ICC system to achieve lower HVAC energy consumption than its conventional counterpart. When q_{CO_2} > 2.78 kWh/kg, the energy required for CO_2 capture becomes dominant, and the ICC system is no longer able to reduce total energy consumption compared to the conventional system.

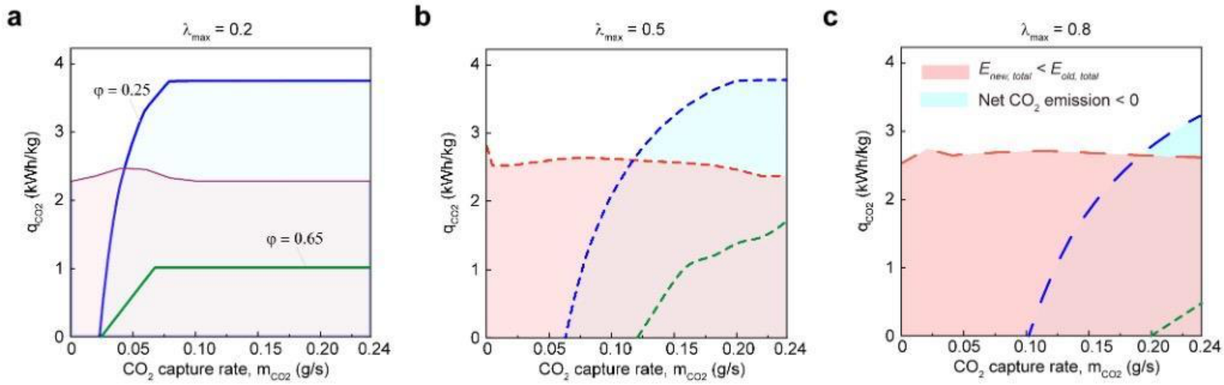

Figure 13. Phase map for negative net CO_2 emissions under the influence of CO_2 capture rate and specific energy consumption of CO_2 capture methods, with different occupancy levels: a, λ_{max} = 0.2; b, λ_{max} = 0.5; c, λ_{max} = 0.8.

For the objective of m_{net,CO_2}< 0, a lower occupancy level (smaller λ_{max}) broadens the feasible region where both objectives can be met. For example, at λ_{max} = 0.2, the feasible values for $\dot{m}_{CO_2}$ and q_{CO_2} range from 0.02 ~ 0.24 g/s and 0 ~ 2.5 kWh/kg, respectively (Figure 13a). In contrast, for λ_{max} = 0.5. the feasible ranges for $\dot{m}_{CO_2}$ narrows down to 0.06~0.24 g/s (Figure 13b), and for λ_{max} = 0.8, the feasible ranges of $\dot{m}_{CO_2}$ and q_{CO_2} narrow further to 0.10~0.24 g/s (Figure 13c). Notably, for λ_{max} = 0.2, increasing $\dot{m}_{CO_2}$ beyond 0.08 g/s does not further expand the feasible range for q_{CO_2}, suggesting an optimal value for $\dot{m}_{CO_2}$ that minimizes ICC's energy consumption, while still yielding a negative CO_2 emissions. Compared to that of φ = 0.65 kg/kWh, the viable range, specifically the m_{net,CO_2} < 0 of the φ = 0.65 is narrower. These phase maps highlight the importance of selecting ICC methods for occupancy levels to maximize both energy savings and decarbonization benefits.

5. CONCLUSION

To optimize and generalize ICC system designs, this study systematically evaluated the performances of an indoor CO_2 capture system in reducing building HVAC energy consumption and carbon emissions, under the influences of climate conditions, occupancy levels, and CO_2 capture methods. Major conclusions include:

1. The ICC system's energy-saving and decarbonization performances vary by month, depending on climate conditions. In months with higher HVAC loads, such as winter months like January and December, the ICC system yields the highest energy saving of 65.8%. In the summer months, it yields an average energy-saving potential of 37.9%. Across all months, the annual average energy-saving potential is 28.5%. Regarding decarbonization potential, ICC yields annual negative carbon emissions, due to its combined advantage of reducing HVAC energy consumption and directly capturing indoor CO_2.
2. Regarding total energy consumption, there exists an optimal CO_2 capture rate that minimizes energy use. While increasing the CO_2 capture reduces HVAC energy consumption, it also increases the energy demand of the ICC system. For λ_{max} =0.5, the optimal CO_2 capture rate is around 0.18 g/s. Regarding net CO_2 emission, a higher CO_2 capture rate leads to greater decarbonization potential, but the benefits plateau as the rate increases further, due to the additional carbon emission associated with ICC operation.

3. The ICC system saves more HVAC energy and captures more CO_2 in crowded indoor environments, and the performances depend on the selection of q_{CO_2} and $\dot{m}_{CO_2}$ simultaneously. The feasible phase maps for each occupancy level have also been obtained, identifying the operating regions that satisfy energy and carbon objectives.

Overall, this study demonstrates the promising potential of ICC systems for decarbonizing buildings, especially in crowded environments and regions with high HVAC loads. Future work should focus on developing high-capacity indoor CO_2 capture materials, smart operation control platforms, and conducting comprehensive life cycle assessments that account for the embodied carbon in materials, manufacturing, maintenance, and end-of-life recycling of the ICC system. Furthermore, a comprehensive economic analysis is essential for practical ICC implementation, including the prediction of payback period, assessment of economic benefits from electricity savings and captured CO_2, and evaluation of costs associated with the ICC system. These efforts will advance the practicality of this technology for developing low-carbon buildings and reducing urban carbon emissions.

AUTHOR CONTRIBUTIONS

Yongting Shen: Conceptualization, Software, Investigation, Validation, Visualization, Formal analysis, Writing. **Hongxing Yang**: Writing, Investigation, Supervision, Funding acquisition.

COMPETING INTERESTS

The authors declare that they have no known competing financial interests or personal relationships that could have appeared to influence the work reported in this paper.

DATA ACCESSIBILITY

Data will be made available on request.

REFERENCES

ASHRAE 62.1, 2010. Ventilation for acceptable indoor air quality. American Society of Heating, Refrigerating and Air Conditioning Engineers.

Department of Climate Change, Energy, the Environment and Water, 2013. HVAC factsheet - Energy breakdown [Online]. Australia: Department of the Environment and Energy. Available: https://www.environment.gov.au/system/files/energy/files/hvac-factsheet-energy-breakdown.pdf [Accessed].

Ministry of Ecology and Environment of the People's Republic of China 2024. Announcement on the Release of the 2022 Electricity CO_2 Emission Factors. In: Ministry Of Ecology And Environment Of The People's Republic Of China (ed.).

Our World in Data, 2023. Carbon dioxide emissions factors [Online]. Available: https://ourworldindata.org/grapher/carbon-dioxide-emissions-factor [Accessed January 01 2025].

Adhikary, S. K., Ashish, D. K. & Rudžionis, Ž. 2021. Aerogel based thermal insulating cementitious composites: A review. Energy and Buildings, 245. DOI: https://doi.org/10.1016/j.enbuild.2021.111058.

Alim, M. A., Tao, Z., Abden, M. J., Rahman, A. & Samali, B. 2020. Improving performance of solar roof tiles by incorporating phase change material. Solar Energy, 207, 1308–1320. DOI: doi.org/10.1016/j.solener.2020.07.053.

Baciocchi, R., Storti, G. & Mazzotti, M. 2006. Process design and energy requirements for the capture of carbon dioxide from air. Chemical Engineering and Processing: Process Intensification, 45, 1047–1058. DOI: https://doi.org/10.1016/j.cep.2006.03.015.

Baus, L. & Nehr, S. 2022. Potentials and limitations of direct air capturing in the built environment. Build. Environ., 208. DOI: https://doi.org/10.1016/j.buildenv.2021.108629.

Buker, M. S. & Riffat, S. B. 2015. Building integrated solar thermal collectors – A review. Renewable and Sustainable Energy Reviews, 51, 327–346. DOI: https://doi.org/10.1016/j.rser.2015.06.009.

Cheng, H.-H. & Tan, C.-S. 2011. Removal of CO_2 from indoor air by alkanolamine in a rotating packed bed. Sep. Purif. Technol., 82, 156–166. DOI: https://doi.org/10.1016/j.seppur.2011.09.004.

Christoph Beuttler, G. H., Ronald Chance 2021. Direct air capture. IEA.

Chu, Y., Xu, P., Jia, Y., Lin, M., Peng, C. & Dou, Q. 2021. An adsorption-based CO_2 treatment unit for ultra-low fresh air HVAC system using solid amine. Energy Build., 247, 111148. DOI:

https://doi.org/10.1016/j.enbuild.2021.111148.
Deutz, S. & Bardow, A. 2021. Life-cycle assessment of an industrial direct air capture process based on temperature–vacuum swing adsorption. Nature Energy, 6, 203–213. DOI: https://doi.org/10.1038/s41560-020-00771-9.
Emmerich, S. J. & Persily, A. K. 2001. State-of-the-art review of CO_2 demand controlled ventilation technology and application. In: COMMERCE, U. S. D. O. (ed.).
Fajardy, M., Chiquier, S. & Mac Dowell, N. 2018. Investigating the BECCS resource nexus: delivering sustainable negative emissions. Energy Environ. Sci., 11, 3408–3430. DOI: https://doi.org/10.1039/C8EE01676C.
Goeppert, A., Czaun, M., Surya Prakash, G. K. & Olah, G. A. 2012. Air as the renewable carbon source of the future: an overview of CO_2 capture from the atmosphere. Energy Environ. Sci., 5, 7833–7853. DOI https://doi.org/10.1039/C2EE21586A.
Grande, C. A. 2022. Modelling of adsorption technologies for controlling indoor air quality. Adsorption, 28, 1–13.
Gu, C., Tan, P., Jiang, T. Y., Wang, X. Q., Hu, B., Liu, X. Q. & Sun, L. B. 2022. Solar-radiation-induced adsorption/desorption system for carbon dioxide capture. Cell Rep., 3, 101122. DOI: https://doi.org/10.1016/j.xcrp.2022.101122.
Harrouz, J. P., Ghali, K., Hmade, M. & Ghaddar, N. 2022a. Carbon capture from indoor air as an alternative ventilation technique. REHVA 14th HVAC World Congress. The Netherlands. DOI: https://doi.org/10.34641/clima.2022.49.
Harrouz, J. P., Ghali, K., Hmadeh, M., Ghaddar, N. & Ghani, S. 2022b. Feasibility of MOF-based carbon capture from indoor spaces as air revitalization system. Energy & Buildings, 255. DOI: https://doi.org/10.34641/clima.2022.49.
Harrouz, J. P., Karam, J., Ghali, K. & Ghaddar, N. 2023. Personalized ventilation with embedded air treatment system for simultaneous cooling and sorption-based carbon and humidity capture. Energy Conversion and Management, 291. DOI: https://doi.org/10.1016/j.enconman.2023.117290.
IEA. 2025. Tracking buildings [Online]. Available: https://www.iea.org/energy-system/buildings [Accessed 09/22 2025].
Isobe, J., Henson, P., Macknight, A., Yates, S., Schuck, D. & Winton, D. Carbon dioxide removal technologies for space vehicles - Past, present, and future. 46th International Conference on Environmental Systems, 10–14 July 2016, 2016 Vienna, Austria.
Jacobson, T. A., Kler, J. S., Hernke, M. T., Braun, R. K., Meyer, K. C. & Funk, W. E. 2019. Direct human health risks of increased atmospheric carbon dioxide. Nature Sustainability, 2, 691–701. DOI: https://doi.org/10.1038/s41893-019-0323-1.
Jelle, B. P. 2011. Traditional, state-of-the-art and future thermal building insulation materials and solutions – Properties, requirements and possibilities. Energy and Buildings, 43, 2549–2563. DOI: https://doi.org/10.1016/j.enbuild.2011.05.015.
Keith, D. W., Holmes, G., St. Angelo, D. & Heidel, K. 2018. A Process for Capturing CO_2 from the Atmosphere. Joule, 2, 1573–1594. DOI: https://doi.org/10.1016/j.joule.2018.05.006.
Kim, M., Kim, H. S., Kim, S., Wee, H., Koh, Y., Kim, K., Lee, M. K., Lee, J. W. & Kang, Y. T. 2025. Indoor CO_2 capture driven energy load reduction and ventilation management for plus energy building applications. Energy, 326. DOI: https://doi.org/10.1016/j.energy.2025.136259.
Kim, M., Lee, J. W., Kim, S. & Kang, Y. T. 2022. CO_2 adsorption on zeolite 13X modified with hydrophobic octadecyltrimethoxysilane for indoor application. J. Clean. Prod., 337, 130597. DOI: https://doi.org/10.1016/j.jclepro.2022.130597.
Kim, M. K., Baldini, L., Leibundgut, H., Wurzbacher, J. A. & Piatkowski, N. 2015. A novel ventilation strategy with CO_2 capture device and energy saving in buildings. Energy and Buildings, 87, 134–141. DOI: https://doi.org/10.1016/j.enbuild.2014.11.017.
Kim, S., Kim, M., Jang, K., Yoon, S. S., Choi, W., Lee, H., Shim, J. H. & Kang, Y. T. 2024. Indoor CO_2 capture-driven passive cooling for photovoltaics with ventilation energy reduction utilizing amine-functionalized adsorbents. Energy Conversion and Management, 307, 118351. DOI: https://doi.org/10.1016/j.enconman.2024.118351.
Kim, S., Kim, M., Xu, R., Park, J. H., Lee, J. W. & Kang, Y. T. 2021. Nano-encapsulated solvent via pickering emulsion in NaOH aqueous solution for indoor CO_2 capture. J. CO2 Util., 51, 101637. DOI: https://doi.org/10.1016/j.jcou.2021.101637.
Kim, S., Kim, M., Xu, Z., Wang, R. & Kang, Y. T. 2023. Hybrid energy-harvesting device driven by membrane-based CO_2 capture. Cell Reports Physical Science, 4. DOI: https://doi.org/10.1016/j.xcrp.2023.101698.
Lee, J. W., Kim, M., Jung, H. S., Xu, R., Kim, S. & Kang, Y. T. 2021. Liquid-like adsorbent assembled by CNTs: Serving as renewable CO_2 capture materials for indoor air. J. Energy Chem., 63, 574–584. DOI: https://doi.org/10.1016/j.jechem.2021.08.027.
Lee, S. C., Hsieh, C. C., Chen, C. H. & Chen, Y. S. 2013. CO_2 adsorption by Y-Type zeolite impregnated with amines in indoor air. Aerosol and Air Quality Research, 13, 360–366. DOI: https://doi.org/10.4209/aaqr.2012.05.0134.
Li, H., Tang, Z., Li, N., Cui, L. & Mao, X.-Z. 2020a. Mechanism and process study on steel slag enhancement for CO_2 capture by seawater. Applied Energy, 276. DOI: https://doi.org/10.1016/j.apenergy.2020.115515.
Li, X., Peng, C. & Liu, L. 2020b. Experimental study of the thermal performance of a building wall with vacuum insulation panels and extruded polystyrene foams. Applied Thermal Engineering, 180. DOI: https://doi.org/10.1016/j.applthermaleng.2020.115801.

Lu, T., Lü, X. & Viljanen, M. 2011. A novel and dynamic demand-controlled ventilation strategy for CO_2 control and energy saving in buildings. Energy and Buildings, 43, 2499–2508. DOI: https://doi.org/10.1016/j.enbuild.2011.06.005.

Lu, X., Pang, Z., Fu, Y. & O'neill, Z. 2022. Advances in research and applications of CO_2-based demand-controlled ventilation in commercial buildings: A critical review of control strategies and performance evaluation. Building and Environment, 223. DOI: https://doi.org/10.1016/j.buildenv.2022.109455.

Meinardi, F., Bruni, F. & Brovelli, S. 2017. Luminescent solar concentrators for building-integrated photovoltaics. Nature Reviews Materials, 2, 17072. DOI: https://doi.org/10.1038/natrevmats.2017.72.

Melikov, A. K., Cermak, R. & Majer, M. 2002. Personalized ventilation evaluation of different air terminal devices. Energy and Buildings, 34, 829–836. DOI: https://doi.org/10.1016/S0378-7788(02)00102-0.

Mertens, J., Breyer, C., Arning, K., Bardow, A., Belmans, R., Dibenedetto, A., Erkman, S., Gripekoven, J., Léonard, G., Nizou, S., Pant, D., Reis-Machado, A. S., Styring, P., Vente, J., Webber, M. & Sapart, C. J. 2023. Carbon capture and utilization: More than hiding CO_2 for some time. Joule, 7, 442–449. DOI: https://doi.org/10.1016/j.joule.2023.01.005.

Park, J., Chae, Y. S., Kang, D. W., Kang, M., Choe, J. H., Kim, S., Kim, J. Y., Jeong, Y. W. & Hong, C. S. 2021. Shaping of a metal-organic framework-polymer composite and its CO_2 adsorption performances from humid indoor air. ACS Appl. Mater. Interfaces, 13, 25421–25427. DOI: doi.org/ 10.1021/acsami.1c06089.

Peng, Y., Fan, L., Jin, W., Ye, Y., Huang, Z., Zhai, S., Luo, X., Ma, Y., Tang, J., Zhou, J., Greenburg, L. C., Majumdar, A., Fan, S. & Cui, Y. 2021. Coloured low-emissivity films for building envelopes for year-round energy savings. Nature Sustainability, 5, 339–347. DOI: https://doi.org/10.1038/s41893-021-00836-x.

Prajapati, A., Sartape, R., Rojas, T., Dandu, N. K., Dhakal, P., Thorat, A. S., Xie, J., Bessa, I., Galante, M. T., Andrade, M. H. S., Somich, R. T., Rebouças, M. V., Hutras, G. T., Diniz, N., Ngo, A. T., Shah, J. & Singh, M. R. 2022. Migration-assisted, moisture gradient process for ultrafast, continuous CO_2 capture from dilute sources at ambient conditions. Energy Environ. Sci., 15, 680–692. DOI: https://doi.org/10.1039/D1EE03018C.

Rajan, P. E., Krishnamurthy, A., Morrison, G. & Rezaei, F. 2017. Advanced buffer materials for indoor air CO_2 control in commercial buildings. Indoor Air, 27, 1213–1223. DOI: https://doi.org/10.1111/ina.12386.

Sabatino, F., Mehta, M., Grimm, A., Gazzani, M., Gallucci, F., Kramer, G. J. & Van Sint Annaland, M. 2020. Evaluation of a direct air capture process combining wet scrubbing and bipolar membrane electrodialysis. Industrial & Engineering Chemistry Research, 59, 7007–7020. DOI: doi.org/10.1021/acs.iecr.9b05641.

Sanz-Perez, E. S., Murdock, C. R., Didas, S. A. & Jones, C. W. 2016. Direct capture of CO_2 from ambient air. Chem. Rev., 116, 11840–11876. DOI: doi.org/10.1021/acs.chemrev.6b00173.

Seok Chae, Y., Park, S., Won Kang, D., Won Kim, D., Kang, M., San Choi, D., Hyeak Choe, J. & Seop Hong, C. 2021. Moisture-tolerant diamine-appended metal–organic framework composites for effective indoor CO2 capture through facile spray coating. J. Chem. Eng., 433, 133856. DOI: https://doi.org/10.1016/j.cej.2021.133856.

Shen, Y., Wang, Q., Lu, L. & Yang, H. 2024. Recent progress in indoor CO_2 capture for urban decarbonization. Nat. Cities, 1, 501–511. DOI: https://doi.org/10.1038/s44284-024-00094-w.

Shen, Y. & Yang, H. 2022. Achieving reduced emission and enhanced air quality by designing a solar-driven indoor CO_2 capture system. J. Clean. Prod., 379. DOI: https://doi.org/10.1016/j.jclepro.2022.134869.

Shen, Y. & Yang, H. 2023. Global performance analysis of a solar-driven indoor CO_2/H_2O capture system for air quality enhancement and cooling energy saving. Energy Convers. Manag., 280, 116831. DOI: https://doi.org/10.1016/j.enconman.2023.116831.

Shindell, D. & Rogelj, J. 2025. Preserving carbon dioxide removal to serve critical needs. Nat. Clim. Change., 15, 452–457. DOI: https://doi.org/10.1038/s41558-025-02251-y.

Siegelman, R. L., Kim, E. J. & Long, J. R. 2021. Porous materials for carbon dioxide separations. Nat. Mater., 20, 1060–1072. DOI: https://doi.org/10.1038/s41563-021-01054-8.

Sinha, A., Thakkar, H., Rezaei, F., Kawajiri, Y. & Realff, M. J. 2022. Reduced building energy consumption by combined indoor CO_2 and H_2O composition control. Applied Energy, 322. DOI: https://doi.org/10.1016/j.apenergy.2022.119526.

Steinemann, A., Wargocki, P. & Rismanchi, B. 2017. Ten questions concerning green buildings and indoor air quality. Build. Environ., 112, 351–358. DOI: https://doi.org/10.1016/j.buildenv.2016.11.010.

Terlouw, T., Treyer, K., Bauer, C. & Mazzotti, M. 2021. Life cycle assessment of direct air carbon capture and storage with low-carbon energy sources. Environ Sci Technol. DOI: doi.org/10.26434/chemrxiv.14346182.

Thakkar, H., Eastman, S., Hajari, A., Rownaghi, A. A., Knox, J. C. & Rezaei, F. 2016. 3D-Printed zeolite monoliths for CO_2 removal from enclosed environments. ACS Appl. Mater. Interfaces, 8, 27753–27761. DOI: https://doi.org/10.1021/acsami.6b09647.

Tian, H., Zhu, L., Ni, J., Wei, T., Wang, P., Xiao, H. & Chen, X. 2023. Indoor CO_2 removal: decentralized carbon capture by air conditioning. Materials Today Sustainability, 22. DOI: https://doi.org/10.1016/j.mtsust.2023.100369.

Wang, S., Bai, X., Zhang, X., Reis, S., Chen, D., Xu, J. & Gu, B. 2021. Urbanization can benefit agricultural production with large-scale farming in China. Nature Food, 2, 183–191. DOI: https://doi.org/10.1038/s43016-021-00228-6.

Wang, W., Wang, J., Chen, J., Huang, G. & Guo, X. 2018. Multi-zone outdoor air coordination through Wi-Fi probe-based occupancy sensing. Energy and Buildings, 159, 495–507. DOI: https://doi.org/10.1016/j.enbuild.2017.11.041.

Yoo, S. Y., Kim, Y. J., Lee, T. H., Lee, B. K., Kim, M. J., Han, S. H., Ha, S. Y. & Park, H. B. 2023. Membrane system for management and utilization of indoor CO_2. Journal of Industrial and Engineering Chemistry, 122, 161–168. DOI: https://doi.org/10.1016/j.jiec.2023.02.018.

Youngmin Cho, S.-B. K., Duck-Shin Park, Woo-Sung Jung, Seung-Woo Hong 2013. Study on the adsorptive removal of indoor CO_2 of car running in downtown area. 2013 ASHRAE Annual Conference.

Zhai, Y., Ma, Y., David, S. N., Zhao, D., Lou, R., Tan, G., Yang, R. & Yin, X. 2017. Scalable-manufactured randomized glass-polymer hybrid metamaterial for daytime radiative cooling. Science, 355, 1062–1066. DOI: doi.org/10.1126/science.aai7899.

Zhu, X., Ge, T., Yang, F. & Wang, R. 2021. Design of steam-assisted temperature vacuum-swing adsorption processes for efficient CO_2 capture from ambient air. Renewable and Sustainable Energy Reviews, 137. DOI: https://doi.org/10.1016/j.rser.2020.110651.

Zuo, J. & Zhao, Z.-Y. 2014. Green building research–current status and future agenda: A review. Renewable and Sustainable Energy Reviews, 30, 271–281. DOI: https://doi.org/10.1016/j.rser.2013.10.021.